Hydrol. Earth Syst. Sci. Discuss., 8, 7137–7175, 2011
www.hydrol-earth-syst-sci-discuss.net/8/7137/2011/
doi:10.5194/hessd-8-7137-2011

Hydrology and
Earth System
Sciences
Discussions

Suspended sediment fluxes in an Indonesian river draining a rainforested basin subject to land cover change

F. A. Buschman[1], **A. J. F. Hoitink**[1,2], **S. M. de Jong**[1], **and P. Hoekstra**[1]

[1]Institute for Marine and Atmospheric research Utrecht (IMAU), Department of Physical Geography, Faculty of Geosciences, Utrecht University, The Netherlands
[2]Hydrology and Quantitative Water Management Group, Department of Environmental Sciences, Wageningen University, The Netherlands

Received: 8 July 2011 – Accepted: 19 July 2011 – Published: 20 July 2011

Correspondence to: F. A. Buschman (frans.buschman@gmail.com)

Published by Copernicus Publications on behalf of the European Geosciences Union.

Abstract

Forest clearing for reasons of timber production, open pit mining and the establishment of oil palm plantations generally results in excessively high sediment loads in the tropics. The increasing sediment fluxes pose a threat to coastal marine ecosystems such as coral reefs. This study presents observations of suspended sediment fluxes in the Berau river (Indonesia), which debouches into a coastal ocean that can be considered the preeminent center of coral diversity. The Berau is an example of a small river draining a mountainous, relatively pristine basin that receives abundant rainfall. Flow velocity was measured over a large part of the river width at a station under the influence of tides, using a Horizontal Acoustic Doppler Current Profiler (HADCP). Surrogate measurements of suspended sediment concentration were taken with an Optical Backscatter Sensor (OBS). Tidally averaged suspended sediment concentration increases with river discharge, implying that the tidally averaged suspended sediment flux increases non-linearly with river discharge. Averaged over the 6.5 weeks observations covered by the benchmark survey, the tidally averaged suspended sediment flux was estimated at 2 Mt y^{-1}. Considering the wet conditions during the observation period, this figure may be considered as an upper limit of the yearly averaged flux. This flux is significantly smaller than what could have been expected from the characteristics of the catchment. The consequences of ongoing clearing of rainforest were explored using a plot scale erosion model. When rainforest, which still covered 50–60 % of the basin in 2007, is converted to production land, soil loss is expected to increase with a factor between 10 and 100. If this soil loss is transported seaward as suspended sediment, the increase in suspended sediment flux in the Berau river would impose a severe sediment stress on the global hotspot of coral reef diversity. The impact of land cover changes will largely depend on the degree in which the Berau estuary acts as a sediment trap.

1 Introduction

Indonesia is the country with the largest marine areas hosting coral reefs, where the center of diversity of several groups of marine organisms is situated (Tomascik et al., 1997; Spalding et al., 2001). At the same time, sediment fluxes from Indonesian islands are disproportionally large. Although the Indonesian Archipelago accounts for only about 2 % of the land area draining into the global ocean, it is responsible for 13 to 18 % of the global sediment transfer to the oceans (Milliman et al., 1999; Syvitski et al., 2005; Milliman and Farnsworth, 2011). The disproportionally high sediment load from the Indonesian islands is due to the high topographical relief, the small size of the drainage basins with easily eroding rocks and heavy rainfall that charactizes the tropics (Milliman et al., 1999). Sediment fluxes in Indonesia are increasing at a higher rate than in other tropical regions, because of large-scale deforestation (Syvitski et al., 2005). The increasing sediment loads pose a serious threat to coastal coral reef ecology (Edinger et al., 1998; Spalding et al., 2001; Fabricius, 2005).

Edinger et al. (1998) found a 30–60 % reduction of coral species diversity at land-affected reefs over a period of 15 yr in Indonesia. The observed reef degradation is partly due to the enlarged sediment fluxes. Turbidity reduces photosynthesis and reduces the maximal depth where corals can survive (Rogers, 1990; Fabricius, 2005). Both turbidity and sedimentation have negative effects on coral reproduction, growth and survival, which may result in decreasing species richness (Fabricius, 2005).

The geography of turbidity may result in a zonation of coral reefs (McLaughlin et al., 2003). In an embayment on Jamaica, Mallela et al. (2004) observed a clear increase of coral reef diversity with distance from the river mouth, which is exemplary for marginal reef systems in general. The geography of turbidity of an Indonesian embayment hosting coral reefs was studied by Hoitink and Hoekstra (2003) and Hoitink (2004), who found that turbidity levels bear a complex relation to the tidal motion and to flows driven by monsoons, and may peak above reef slopes as a result of cloud formation.

Despite the apparent impacts of sediment fluxes on coral reefs, sediment fluxes in Indonesian rivers are rarely being monitored continuously. This paper presents continuous observations of flow and suspended sediment concentration in the Berau river situated in Kalimantan, Indonesia (Fig. 1). The Berau catchment can be considered relatively pristine, with 50–60 % of the land surface being covered by rainforest in 2007 (Ekadinata et al., 2010). Especially the lowland and swamp forest support high densities of the Bornean orangutan (Marshall et al., 2007). The adjacent Berau continental shelf is host to an extremely diverse coral community (de Voogd et al., 2009) that shows a marked zonation with more turbid reefs west of the Derawan reef chain and oceanic reefs east of the chain (Fig. 1). Furthermore, the continental shelf is of global interest due to the presence of several anchialine lakes and for its nesting grounds for the endangered green sea turtle (Tomascik et al., 1997; de Voogd et al., 2009). The coastal oceanography of the Berau continental shelf was studied by Tarya et al. (2010, subm), who revealed the spatial structure of the river plume and underlying governing processes. Sediments that are suspended in the river plume may be transported to the reefs, whereas sediment that is transported as bed load deposits primarily near the channel mouths and forms mouth bars.

The present study serves as a benchmark reference for suspended sediment fluxes to the Berau coastal shelf for the situation in 2007, when the catchment was relatively pristine and anthropogenic disturbance was increasing rapidly. A simple erosion model is employed only to investigate the sensitivity of suspended sediment fluxes on land cover changes, which include forest clearing for timber production, open pit mining and conversion into oil palm plantations.

This paper continues with the *field site*, where details of the geology, climate and other characteristics of the Berau basin are given. In the subsequent section the *methods* are described, including the calibrations necessary to obtain suspended sediment concentration and discharge. In the *observations* section the tidally averaged suspended sediment concentrations are shown and discussed. In the subsequent section, the *sensitivity of tidally averaged suspended sediment flux to land cover* are investigated by means of the erosion model. A *discussion* on the observed sediment flux and the *conclusions* complete this paper.

2 Field site

2.1 Geology and resources

The Berau district, which encloses the Berau catchment, is situated on the Sunda plate. The Sunda plate is an extension of mainland southeast Asia that was uplifted and folded in the Tertiary (65–3 million years ago), associated with the northward movement of the Australian plate (MacKinnon et al., 1996). This tectonic movement created the topography of Borneo, including the high mountain range in central Borneo and the surrounding hilly landscape. Erosion of this mountain range over a period of about 15 million years has resulted in thick sedimentary deposits in basins, such as the Berau-Bulungan basin (Mantel, 2001). This basin contains pools of coal, gass and oil (Voss, 1982), which are important for the district economically. Gold panning is of local economic importance in the Berau district.

The dominant source rocks for soils in Borneo are sedimentary. Active volcanoes that are typical for most other Indonesian islands are absent in Kalimantan, the Indonesian part of the island Borneo. Sedimentary rocks are generally poor in weatherable minerals and rich in silica. When such sedimentary parent rocks are well drained, red-yellow podzolic soils develop, of which Ultisols are the dominant type (MacKinnon et al., 1996). Ultisols are usually very deep, poorly fertile and aluminium toxic soils, which limits their use for crop production and makes them vulnerable for erosion (Mantel, 2001). Ultisols cover most of the Berau district. In the south of the district a more fertile limestone area occurs (Voss, 1982). The karst formations, caves and limestone rainforests in this area are considered as one of the most valuable areas of Indonesia for conservation (MacKinnon et al., 1996).

The rainforest cover in the Berau district is rapidly decreasing (Table 1). Since the area of the Berau catchment is 55 % of the whole Berau district area, Table 1 is indicative for the Berau catchment. In the period between 2005 and 2008, which encloses the period of our fieldwork, the total forest cover decreased with about 40 %. In 2007, when most of the observations for this study were made, the total forest cover in the Berau catchment was still about 50–60 %. This forest cover is still relatively high for Indonesia, since logging of the rainforests occurs at large scale, both legally and especially from 1998 onwards illegally (Casson and Obidzinski, 2002). The logging yields timber, which is an important resource for the Berau district, and may be associated with establishing oil palm plantations. As a result of the logging, soil erosion rates increase dramatically (El-Hassanin et al., 1993; Moehansyah et al., 2004) and also sediment fluxes towards the sea may increase substantially.

2.2 Climate

The mean annual rainfall at Tanjung Redeb measured 2105 mm over the observation period from 1987 to 2007. In this period, rainforest clearing has occurred, which may result in decreasing rainfall (Bruijnzeel, 2004). Time series of rainfall did not show such a decreasing trend. During the El Niño period of 1997 and 1998 and the La Niña period of 1999, rainfall over Kalimantan was respectively lower and higher than average. These differences were not so pronounced at the meteorological station in the harbor town of Tanjung Redeb. Since the meteorological data was collected 20 m above mean sea level and rainfall is generally correlated with the altitude, the station may slightly underpredict the rainfall in the Berau catchment. Spatial patterns of rainfall show to be minimal at Tanjung Redeb, and are maximally 2.2 times higher at the highest altitudes in the Berau catchment (Voss, 1982).

Figure 2 shows a rainfall climatology for the Berau catchment, which shows characteristics of two of the three climatic regions in Indonesia as defined by Aldrian and Susanto (2003). The region that covers large parts of southern Indonesia experiences a strong influence of the wet Northwest Monsoon from November to March and of the dry Southeast Monsoon from May to September. In the second region, that is centered in western Indonesia, the Monsoons are suppressed, resulting in small differences between the wet and dry seasons (Aldrian and Susanto, 2003). In the Berau catchment the variation in monthly rainfall reflects both these climatic regions. The variation within a year is similar as in the first climatic region, whereas the difference between the wet and dry periods is limited as in the second.

2.3 The Berau river

The Berau river is formed just upstream of the village of Gunung Tabur, where two rivers join (Fig. 1). The drainage basin of the Berau river is situated in between the larger drainage basins of the Kayan and the Mahakam rivers that also run in eastward direction. These two large rivers drain the highest mountains of central Kalimantan. The size of the Berau catchment is about 12 000 km^2 and the highest altitude is about 1800 m, which reveals the mountainous character of the Berau catchment.

The Berau river discharge at Gunung Tabur averaged 605 m^3 s^{-1} during several months in 2007 (Buschman et al., 2009), which was an average year in terms of rainfall. At Gunung Tabur, the tidal regime is mixed, predominantly semidiurnal. The tidal range is about 1 m during neap tide and 2.5 m during spring tide, which is similar to the coastal conditions. The cross sectional area of the Berau river increases more or less exponentially going seaward (Buschman et al., 2009), which is associated with the increasing tidal prism.

The bathymetry around Gunung Tabur, where instruments were mounted on an existing wooden jetty, shows several deep troughs in the outer bend of the tidal river. The maximum depth in the cross-section of the wooden jetty was 8 m (Fig. 3). The bathymetry was obtained by sailing transects across the channel at least every 500 m with an echosounder and a GPS, correcting for water level variation, and interpolating along the channel.

3 Methods

3.1 Obtaining continuous discharge

Table 2 gives an overview of the observations taken at Gunung Tabur. We use the same discharge data as analyzed by Buschman et al. (2009), who applied the methods described by Hoitink et al. (2009) to convert HADCP velocity data to discharge (Q). A three-day period of HADCP was added to the data series described in Buschman et al. (2009), during which the protocol was setup to collect the velocity profiles continuously at a higher sampling rate of 2 Hz. The high-frequency data were collected to investigate processes of lateral momentum transfer in a future study, but serve here to complement the data series from Buschman et al. (2009), as they coincide with suspended sediment data series.

3.2 Obtaining profiles of suspended sediment concentration

Vertical profiles of turbidity were measured with an Optical Backscatter (OBS) device every 50 m across the approximately 400 m wide Berau river at Gunung Tabur. Profiles of turbidity were measured covering tidal cycles at neap tide, at spring tide and during an intermediate tidal range in May, and at neap and spring tide in September 2007 (Table 2). In September 2007 about 20 sets of profiles were taken across the river throughout a 12.5 h period, attaining a higher temporal resolution than in May 2007.

Suspended sediment concentration (c) was obtained from turbidity after calibration with in situ water samples. In total 99 water samples were taken simultaneously with turbidity measurements. Half of the samples was taken at 1 m from the bottom and the other half at 1 m from the water surface. For each water sample a known volume of water was filtered through membrane filters with a pore size of about 0.45 µm. Drying the filter in an oven to remove water and organic matter from the residue, weighing the residue and divide this weight by the filtered volume, resulted in the estimate of c. Figure 4 shows the linear regression of c-estimates to optical backscatter in Volts.

Regarding this calibration, 7 of the 99 points were excluded based on a 4-sigma test. The resulting regression has a high correlation (Fig. 4), suggesting that the sediment characteristics were not very different between spring and neap tides and between May and September 2007. The obtained regression coefficients were used to obtain c from the vertical profiles of turbidity.

For the two days of September 2007, which had a higher temporal resolution, the variation of c within the cross section was investigated. The concentration profiles were interpolated to a regular vertical interval of 0.1 m. The top 0.3 m and the bottom 0.5 m were discarded, since these measurements could have been affected by air bubbles or by interference with the bed. The vertical coordinate was expressed in terms of normalized depth (σ), defined as:

$$\sigma = \frac{d+z}{d}, \tag{1}$$

where z is the height from the water surface level and d is the total water depth. All profiles were interpolated on a (n,σ) grid. Finally, a box filter was applied in time and over depth to smooth the data. Figure 5 shows the smoothed suspended sediment concentrations for three moments on each observation day, revealing that suspended sediment concentration varies little over width and depth.

3.3 Obtaining continuous suspended sediment concentration

Turbidity was measured continuously with a 5 minutes interval using a 600 Optical Monitoring Station (OMS) manufactured by YSI. The OMS was deployed at the same jetty as the HADCP at about 1.5 m above the bed and between 2.5 and 4.5 m below the water surface, for several months. Although the optical backscatter sensor was equipped with a wiper and with a cage to protect the sensor, the turbidity signal often contained an increasing number of spurious peaks in each of the time series. The larger part of those peaks were caused by biological fouling, with weeds, algae and shells growing on the instrument. Only two data series with relatively few spurious peaks were sufficiently reliable for analysis. The first of those time series lasted 6.5 weeks and the second time series covered the two days when the high time resolution data were collected (Table 2).

For those two turbidity time series, data processing started by removing the spurious peaks. Turbidity samples exceeding 300 NTU, which were obviously not related to high turbidity, were removed. Next, a moving window filter was applied, retaining the data points within 4 standard deviations from the median obtained over a 24 h period. A last filtering procedure was necessary only for a period between Julian days 538.5 and 542.5, when some of the measured turbidities were high, whereas subsequent observations showed a low value. The highest signal was attributed to biological fouling and these points were removed. The number of points removed from the time series did not exceed 4 % of the total, for each of the two series.

The valid points were interpolated and smoothed on a regular 5 min interval, using the methods of Schlax and Chelton (1992) with an overturning period of 3 hours. The resulting turbidity time series of September 2007 was linearly regressed against the cross section averaged suspended sediment concentration (C) derived from the OBS profiles. Although this approach ignores variation of c over the cross section, Fig. 6 shows that the estimates of C from the OMS turbidity correspond well to the corresponding OBS-derived values. Since the spatial variation of suspended sediment concentration is limited, the point data from the OMS are largely representative for the cross section (Fig. 5).

3.4 Erosion model

The Universal Soil Loss Equation (USLE) is applied to a hillslope that has characteristics typical for the Berau drainage basin. The plot-scale model enables to make a first order assessment of the sensitivity of the sediment flux in the Berau river to land cover changes. The USLE is a widely used soil erosion model (Merritt et al., 2003; Jetten and Favis-Mortlock, 2006; Kinnell, 2010). The USLE is an empirical erosion regression equation based primarily on observations. The annual soil loss per unit area (A_e in

$\mathrm{t\,ha^{-1}\,y^{-1}}$), averaged over a plot on a constant sloping hill is (Wischmeier and Smith, 1978):

$$A_\mathrm{e} = R_\mathrm{e} K S_\mathrm{s} S_\mathrm{l} C_\mathrm{m} P, \tag{2}$$

where R_e is the rainfall erosivity factor ($\mathrm{MJ\,mm\,ha^{-1}\,y^{-1}\,h^{-1}}$), K is the soil erodibility factor ($\mathrm{t\,h\,MJ^{-1}\,mm^{-1}}$), S_s is the slope-steepness factor (–), S_l is the slope-length factor (–), C_m is the cover and management factor (–) and P is the support practices factor (–).

Each factor in the USLE model can be derived or estimated based on physical characteristics of a hillslope. Because no high temporal resolution rainfall data was available for the Berau basin, R_e was estimated from annual precipitation (P in $\mathrm{mm\,y^{-1}}$) according to an empirical relation found for southeastern Australia (Yu and Rosewell, 1996):

$$R_\mathrm{e} = 0.0438 P^{1.61}. \tag{3}$$

This relation is remarkably similar to the empirical relation that Renard and Freimund (1994) found for the United States, which suggests a universal nature of this relationship (Yu and Rosewell, 1996). Considering the small variation between mean monthly rainfall (Fig. 2), estimates of R_e according the annual rainfall can be used to assess the relative soil loss.

The factors S_s and S_l are usually derived jointly as:

$$S_\mathrm{s} S_\mathrm{l} = \left(\frac{L_\mathrm{s}}{22.1}\right)^m (65.41 \sin^2\alpha + 4.56 \sin\alpha + 0.065), \tag{4}$$

where L_s is the length of the slope (m) and m is an exponent between 0.2 and 0.5 depending on α, which represents slope angle here (Wischmeier and Smith, 1978). Equation (4) is the result of a regression of data with slopes in between 2 and 10 degrees.

For the cover and management factor C_m, which is the ratio of the long-term soil loss from a vegetated area to the long-term soil loss from a bare fallow area, values for land cover types that occur in the Berau catchment are given in Table 3.

4 Observations

4.1 Discharge

The flow at Gunung Tabur is bidirectional. Peak discharge magnitudes differ little between flood tide and ebb tide (top panel of Fig. 7). Because ebb usually has a longer duration, a net flow seaward occurs, when averaged over a tidal cycle. The tidally averaged discharge ($\langle Q \rangle$), obtained by applying a running mean over 24.8 h period to time series of discharge, is always positive. The discharge averaged over the full 6.5 weeks shown in Fig. 7 amounted to 703 $m^3 s^{-1}$, whereas it was 605 $m^3 s^{-1}$ averaged over 6 months in the same year (Buschman et al., 2009). The maximum observed tidally averaged discharge was 1412 $m^3 s^{-1}$, which occurred at Julian day 545. During that event, the flow direction was seaward almost over the entire day. The discharge peaked at 2896 $m^3 s^{-1}$, which corresponds to a cross section averaged flow velocity of 1.0 $m s^{-1}$.

The variation of $\langle Q \rangle$ is due to river discharge variations and tidal effects. Around spring tide bottom friction is elevated, which results in a higher tidally averaged water level gradient than at neap tide (Buschman et al., 2009). Due to temporal water storage, the tidally averaged discharge is smaller during periods with increasing water level gradients. The variation of $\langle Q \rangle$ induced by the tides, however, is small with respect to the variation due to river discharge variation from runoff, which is partly caused by the mountainous character of the catchment.

4.2 Suspended sediment concentration

The middle panel of Fig. 7 shows the cross section averaged suspended sediment concentration, estimated from the OMS measurements. Values of C vary considerably over a tidal period. The highest value occurs most often in the ebb phase. The low-frequent variation of C is generally highest around spring tide. The peak value of $C = 0.26\,\mathrm{kg\,m^{-3}}$ coincides with the highest river discharge, at Julian day 545.

4.3 Estimating suspended sediment particle size

Both during spring tide and during neap tide, profiles of c were well-developed (Fig. 5). For those concentration profiles, observed during two days in September 2007, Rouse profiles were fitted, yielding a bulk estimate of the sediment fall velocity (w_s). Rouse profiles represent steady state conditions when downward settling is balanced by upward diffusion of sediment. Under these conditions, c at level $d+z$ above the bed (c_z) relates to the reference concentration (c_ref) at level $d+z_\mathrm{ref}$ according to (Dyer, 1986):

$$c_\mathrm{z} = c_\mathrm{ref}\left(\frac{-z(d+z_\mathrm{ref})}{(d+z)(-z_\mathrm{ref})}\right)^{w_\mathrm{s}/(\beta\kappa u_*)}. \tag{5}$$

The exponent governs the shape of the profile and is named the Rouse parameter. It consists of w_s, shear velocity u_*, the Von Karman constant that has a constant value of 0.4, and β, which is a constant of proportionality between the diffusion coefficients of suspended sediment and water, usually assumed to be unity (Dyer, 1986). Using $d+z_\mathrm{ref} = z_0$ and inferring u_* from the HADCP flow velocity data (Hoitink et al., 2009), w_s and c_ref were derived from a best fit procedure.

The sediment particle diameter (d_s) can be derived from w_s according to the Stokes law (Dyer, 1986):

$$d_\mathrm{s} = \left(\frac{18\mu w_\mathrm{s}}{g(\rho_\mathrm{s}-\rho)}\right)^{0.5}, \tag{6}$$

Title Page
Abstract | Introduction
Conclusions | References
Tables | Figures
◂◂ | ▸▸
◂ | ▸
Back | Close
Full Screen / Esc
Printer-friendly Version
Interactive Discussion

where μ is dynamic viscosity, g is gravitational acceleration, ρ_s is density of the sediment particle and ρ is water density. During spring tide w_s was estimated as $1 \times 10^{-3}\,\mathrm{m\,s^{-1}}$, which corresponds to medium silt with $d_s = 29 \times 10^{-6}\,\mathrm{m}$. During neap tide the variation in c was smaller, resulting in a representative d_s that falls within the clay and fine silt fractions. Both the mean grain size of spring tide and neap tide may be considered relatively fine, explaining the small variation of c over depth (Fig. 5).

4.4 Suspended sediment flux

From Q and C, a first order estimate of the suspended sediment flux (S) can be obtained from:

$$S \approx QC. \tag{7}$$

Given the small variation of c over the cross section (Fig. 5), second order effects are expected to be small. A small bias can be expected from the fact that flow velocity (u) is highest near the surface, where c is lowest, and vice versa near the bed. At the tidal cycle during spring tide variations of c in the vertical are largest, which can be explained from coarser sediment to be brought in suspension at that time. Using logarithmic profiles of u (Hoitink et al., 2009) and the observed c profiles at during spring tide, S was calculated by integrating uc over depth and width. The obtained more accurate estimate of S showed a maximum deviation of 25 % from the corresponding estimate derived from Eq. (7), confirming second order effects to be minor. We choose not to account for the small bias caused by resuspension near the bed, since it is unlikely that the coarser sediment eventually will remain suspended once the river effluent reaches the coast, and pose a threat to marine ecosystems.

The instantaneous and tidally averaged peak value of S amount to $730\,\mathrm{kg\,s^{-1}}$ and $270\,\mathrm{kg\,s^{-1}}$, respectively, which occur during the highest river discharge. Values of S averaged over the full time series amount to and $60\,\mathrm{kg\,s^{-1}}$, or $2\,\mathrm{Mt\,y^{-1}}$. Lane et al. (1997) and French et al. (2008) stress that it is difficult to obtain a reliable estimate of tidally averaged S in a tidal river, since tidally averaged S is often only a small fraction of the instantaneous peak values. In the Berau river, tidally averaged values of S exceed 20 % of the instantaneous peak value of S, which places this general view in perspective. The underlying reason is that the tidal curves are not a superposition of a simple harmonic and a constant, representing discharge, which would result in peak ebb currents being much larger than peak flood currents. Instead, the duration of the ebb phase is longer to account for the river discharge, while peak ebb currents and peak flood currents are similar.

4.5 Variation of tidally averaged *S*

Figure 7 showed that tidally averaged S was always directed seawards during the 6.5-weeks observation period. The variation in tidally averaged S may be due to variations of $\langle Q \rangle$ and $\langle C \rangle$ or due to variations of C and Q within a tidal cycle (Meybeck et al., 2003):

$$\langle S \rangle = \langle Q \rangle \langle C \rangle + \langle Q' C' \rangle, \tag{8}$$

where the quotes indicate the deviation from the tidal average: $Q' = Q - \langle Q \rangle$ and $C' = C - \langle C \rangle$.

Figure 8 shows that the product $\langle Q \rangle \langle C \rangle$ dominates the dynamics. Tidally averaged discharge and suspended sediment concentration ($\langle Q \rangle$ and $\langle C \rangle$, respectively) are linearly correlated, yielding a skill score of $r^2 = 0.5$. The tidally averaged suspended sediment flux thus increases non-linearly with river discharge. Due to this non-linearity, the period of high tidally averaged S is limited, exceeding 150 kg m^{-3} for only 8 % of the time. Half of the suspended sediment flux is concentrated in only 25 % of time.

The contribution of variations of Q and C within a day only has a small contribution to $\langle S \rangle$, which is highest when variations in C within a day are pronounced (Figs. 7 and 8). Since C is usually elevated more during the peak ebb flows and the ebb duration is longer than flood duration, the correlation term $\langle Q' C' \rangle$ typically results usually in a positive contribution to the seaward directed flux.

4.6 Highest observed tidally averaged S

To analyze the periods with the highest suspended sediment flux, Fig. 9 zooms in on two peak events. The right panels show results from the period with the highest tidally averaged S, occurring at the highest river discharge. The peak flow velocities during ebb are higher than during lower river discharge, implying that also coarser bed particles may be resuspended. As a result, tidally averaged C is also elevated. This elevation, in combination with the high ebb flow velocities and the long ebb periods, result in the highest observed $\langle S \rangle$ of 272 $\mathrm{kg\,s^{-1}}$.

The left panels indicate a period around Julian day 513, when the largest variation in C was observed. At this day the flow velocity amplitude increases, with spring tide occurring three days later. Concurrently, the river discharge increases. During the two ebb periods of this day, C shows peaks that are more than two times higher than the tidally averaged C. These dramatic increases of C are likely related to high sediment discharge events in one of the two rivers that drain into the Berau river. Clouds of sediment may be passing by at Gunung Tabur in the Berau river, remaining unaffected by flow velocity variation.

5 Sensitivity of tidally averaged S to land cover

5.1 Motivation and assumptions

This section describes the application of the erosion model. Conversion of forest to a type of production land results in a significant decrease of protection to soil loss (Sect. 2). On the steep slopes of central Borneo, Besler (1987) estimated that soil loss from hillslopes with bare soil was over 10 000 times larger than losses from forested hillslopes. We use the USLE to investigate effects of land cover changes on a hillslope that has characteristics typical for the Berau drainage basin. Although the model describes plot-scale erosion processes, we assume that the model provides first order estimates of the sensitivity of soil loss to land cover changes in the Berau catchment.

Increasing soil loss also implies elevated suspended sediment concentration in streams and rivers. In the Berau river, sufficient additional sediment transport capacity is available to convey additional sediment input from the catchment to the sea, since conditions are far from supersaturated. Hence, additional soil loss may result in increasing sediment stress on the coral reefs and other marine ecosystems.

5.2 Erosion model results

Table 4 gives an overview of the default input variables for a hillslope that has characteristics typical for the Berau catchment. The erosivity factor R_e results from Eq. (3) using the annual rainfall averaged over the period 1987 to 2007. The soil erodibility factor K for the strongly weathered Ultisols, which are the dominant soil type in the basin, is characterized by $0.013\,\mathrm{t\,h\,MJ^{-1}\,mm^{-1}}$ (Wischmeier and Smith, 1978). The factors S_s and S_l result from Eq. (4), the plot length standard in USLE of 22 m and a slope of 10 degrees that characterizes the rolling plains. The value for C_m (Table 3) represents primary rainforest, which covers a large share of the drainage basin and especially the steeper parts where soil loss is large. Since no erosion protection measures were taken, the support practice factor was set to 1.

The sensitivity of A_e to land cover type appears to be high (Table 5). Annual soil loss from an oil palm plantation is about 50 times higher than from a primary rainforest with further the same conditions. This factor is even higher in comparison with shifting cultivation, which is carried out by the indigenous Dayak population. The soil loss that occurs from bare ground, which represents the areas with open pit mining, is 167 times higher than for primary rainforest land cover. Considering that the rainforest cover was about 50–60 % in 2007, conversion of this rainforest into intensive production land may result in 10–100 times higher soil loss. If this additional sediment is transported to the rivers, suspended sediment fluxes in the Berau river may also increase with a factor 10–100 with respect to the situation in 2007.

6 Discussion

The observed suspended sediment flux averaged $2\,\mathrm{Mt\,y^{-1}}$ during the 6.5 weeks when valid tidally averaged S observations were derived. In this period, rainfall was about two times higher than average at the station of Tanjung Redeb (Table 6). Moreover, rainfall was higher than the average in the wettest three months. Assuming that the station of Tanjung Redeb is indicative for the whole catchment, the observed suspended sediment flux may be considered as an upper limit of the yearly averaged suspended sediment flux.

The calculated fluxes of suspended sediment in the Berau river can be compared with what can be expected from the literature. Based on the maximal figure of the yearly averaged flux, the sediment yield from the Berau catchment is $170\,\mathrm{t\,km^{-2}\,y^{-1}}$. In contrast, Milliman and Farnsworth (2011) estimated that suspended sediment yields in Indonesia, the Phillipines and Taiwan are higher than $1000\,\mathrm{t\,km^{-2}\,y^{-1}}$. This relatively high yield is due to the generally small drainage basin areas, high topographic relief, relatively young and erodible rocks, and heavy rainfall (Milliman et al., 1999). Although the Berau river is an example of such a small river draining a mountainous catchment, even its maximal sediment yield is much lower than $1000\,\mathrm{t\,km^{-2}\,y^{-1}}$. Part of this discrepancy can be explained by the old and deeply weathered rocks in east Borneo (Douglas, 1999). The sediment yield from these Tertiary rocks is about an order of magnitude lower than from tectonically active parts of Indonesia with volcanoes (Douglas, 1999). The sediment yield of the Mahakam river, which also drains to the east coast of Borneo, supports that sediment yield from east Borneo is relatively low for Indonesia. The yield is similar as the figure for the Berau river, being $180\,\mathrm{t\,km^{-2}\,y^{-1}}$ (Storms et al., 2005).

The relatively low sediment yield from the Berau river may also be due to the high degree in which rainforest cover protected the soil against erosion in 2007. The relatively high rainforest cover may also explain the small variation within the observation period. The tidally averaged suspended sediment flux in the Berau river varied between 0.4

and 8.6 Mt y^{-1}. The peak value was only about 4 times higher than the average, which is less than what is found in literature. Douglas et al. (1999) found that in small catchments in Malaysian Borneo, the bulk of suspended sediment transport occurred in only 5 days. Our observations indicate that in relatively pristine and large catchment areas, sediment transport is more equally distributed over the year. From another perspective, the absence of extreme peaks could be the reason for the small overall transport rates.

Over the past decades, the sediment supply of the Berau river has probably increased, since areas covered with rainforest were subjected to land cover types that offer less protection to soil loss. From a comparison of historical and actual bathymetric maps, the morphological changes in the Berau river appeared to be limited, which suggests that the Berau river acts as a conduit of suspended sediment rather than as a trap. The Berau river splits into a channel network (Fig. 1), where accumulation of suspended sediment may occur. A comparison of bathymetric maps revealed that the most northeastern channel of the network has silted up significantly over the past decades (Buschman et al., 2010), which suggests that increased sediment loads may deposit in the estuarine system, rather than being issued to the coastal system.

7 Conclusions

A benchmark study was performed aiming to assess the fluxes of suspended sediment in the Berau river, which is an Indonesian tidal river draining a relatively pristine watershed. The Berau river issues its discharge to the Berau continental shelf, which is an ecological hotspot of global importance. The tidally averaged suspended sediment flux averaged 2 Mt y^{-1} during a 6.5 weeks observation period in 2007. Since the observation period was relatively wet, the figure can be considered as the upper limit of the yearly averaged sediment flux. Comparing this maximal figure divided by the Berau catchment area with other studies, shows that the sediment yield from the Berau catchment is substantially smaller than from other similar tropical catchments. This discrepancy may be explained by the old and deeply weathered parent rock and the still relatively high rainforest cover in 2007, which result in limited soil erosion.

A plot scale erosion model was used to explore the first order response of soil erosion to expected land cover changes. In 2007, the rainforest cover in the Berau basin was 50–60 %, which is high compared to the rest of Indonesia. When this rainforest is converted to production land, such as oil palm plantation, the supply of sediment and associated fluxes of suspended sediment may increase 10–100 times. This increase implies that also tidally averaged suspended sediment flux in the Berau river increases. Whether or not this results in a seaward shift of the zonation of coral reefs observed in the coastal ocean, depends on the degree in which the estuary act as a sediment trap.

Acknowledgements. This study was supported by grant WT 77-203 of WOTRO Science for Global Development, a division of the Netherlands Organisation of Scientific Research (NWO). We acknowledge M. C. G. van Maarseveen (Utrecht University) for preparing and maintaining the instruments and his technical assistance. We thank A. Tarya (Utrecht University) and a number of students from Wageningen University and Utrecht University who assisted during the field campaigns. Theses by K. Wetser and M. Leenheer were used for this study. We thank M. van der Vegt for commenting on an earlier version of this article.

References

Aldrian, E. and Susanto, R. D.: Identification of three dominant rainfall regions within Indonesia and their relationship to sea surface temperature, Int. J. Climatol., 23, 1435–1452, doi:10.1002/joc.950, 2003. 7142, 7143

Besler, H.: Slope properties, slope processes and soil erosion risk in the tropical rain forest of Kalimantan Timur (Indonesian Borneo), Earth Surf. Processes Landforms, 12, 195–204, 1987. 7152, 7163

Bruijnzeel, L. A.: Hydrological functions of tropical forests: not seeing the soil for the trees?, Agric. Ecosyst. Environ., 104, 185–228, Global Workshop on Bringing the Landscape into Focus, Chiang Mai, THAILAND, NOV 12–13, 2001, 2004. 7142

Buschman, F. A., Hoitink, A. J. F., van der Vegt, M., and Hoekstra, P.: Subtidal water level variation controlled by river flow and tides, Water Resour. Res., 45, W10420, doi:10.1029/2009WR008167, 2009. 7143, 7144, 7148

Buschman, F. A., Hoitink, A. J. F., van der Vegt, M., and Hoekstra, P.: Subtidal flow division at a shallow tidal junction, Water Resour. Res., 46, W12515, doi:10.1029/2010WR009266, 2010. 7155

Casson, A. and Obidzinski, K.: From new order to regional autonomy: shifting dynamics of "illegal" logging in Kalimantan, Indonesia, World Development, 30, 2133–2151, 2002. 7142

de Voogd, N. J., Becking, L. E., and Cleary, D. F. R.: Sponge community composition in the Derawan islands, NE Kalimantan, Indonesia, Mar. Ecol. Prog. Ser., 396, 169–180, doi:10.3354/meps08349, 2009. 7140

Douglas, I.: Hydrological investigations of forest disturbance and land cover impacts in South-East Asia: a review, Phil. Trans. R. Soc. Lond. B, 354, 1725–1738, 1999. 7154

Douglas, I., Bidin, K., Balamurungan, G., Chappell, N. A., Walsh, R. P. D., Greer, T., and Sinun, W.: The role of extreme events in the impacts of selective tropical forestry on erosion during harvesting and recovery phases at Danum valley, Sabah, Phil. Trans. R. Soc. Lond. B, 354, 1749–1761, 1999. 7155

Dyer, K. R.: Coastal and estuarine sediment dynamics, Wiley, 1986. 7149

Edinger, E. N., Jompa, J., Limmon, G. V., Widjatmoko, W., and Risk, M. J.: Reef degradation and coral biodiversity in indonesia: Effects of land-based pollution, destructive fishing practices and changes over time, Mar. Pollut. Bull., 36, 617–630, doi:10.1016/S0025-326X(98)00047-2, 1998. 7139

Ekadinata, A., Rahmanulloh, A., Pambudhi, F., Ibrahim, I., van Noordwijk, M., Sofiyuddin, M., Sardjono, M. A., Subekti, R., Dewi, S., Budidarsono, S., and Said, Z.: Carbon Emissions from Land Use, Land Use Change and Forestry (LULUCF) in Berau District East Kalimantan, Indonesia, Tech. rep., ICRAF Southeast Asia, 2010. 7140, 7161

El-Hassanin, A. S., Labib, T. M., and Gaber, E. I.: Effect of vegetation cover and land slope on runoff and soil losses from the watersheds of Burundi, Agric. Ecosyst. Environ., 43, 301–308, doi:10.1016/0167-8809(93)90093-5, 1993. 7142

Fabricius, K. E.: Effects of terrestrial runoff on the ecology of corals and coral reefs: review and synthesis, Mar. Pollut. Bull., 50, 125–146, doi:10.1016/j.marpolbul.2004.11.028, 2005. 7139

French, J. R., Burningham, H., and Benson, T.: Tidal and Meteorological Forcing of Suspended Sediment Flux in a Muddy Mesotidal Estuary, Estuaries Coasts, 31, 843–859, doi:10.1007/s12237-008-9072-5, 2008. 7150

Hoitink, A. J. F.: Tidally-induced clouds of suspended sediment connected to shallow-water coral reefs, Mar. Geol., 208, 13–31, 2004. 7139

Hoitink, A. J. F. and Hoekstra, P.: Hydrodynamic control of the supply of reworked terrigenous sediment to coral reefs in the bay of Banten (NW Java, Indonsesia), Estuarine Coastal Shelf Sci., 58, 743–755, doi:10.1016/S0272-7714(03)00181-1, 2003. 7139

Hoitink, A. J. F., Buschman, F. A., and Vermeulen, B.: Continuous measurements of discharge from a Horizontal ADCP in a tidal river, Water Resour. Res., 45, W11406, doi:10.1029/2009WR007791, 2009. 7144, 7149, 7150

Jetten, V. and Favis-Mortlock, D.: Soil erosion in Europe, p. chapter 50, John Wiley and sons, doi:10.1002/0470859202.ch50, 2006. 7146

Kinnell, P. I. A.: Event soil loss, runoff and the Universal Soil Loss Equation family of models: A review, J. Hydrol., 385, 384–397, doi:10.1016/j.jhydrol.2010.01.024, 2010. 7146

Lane, A., Prandle, D., Harrison, A. J., Jones, P. D., and Harvis, C. J.: Measuring fluxes in tidal estuaries: sensitivity to instrumentation and associated data analyses, Estuarine Coastal Shelf Sci., 45, 433–451, 1997. 7150

MacKinnon, K., Hatta, G., Halim, H., and Mangalik, A.: The ecology of Kalimantan; Indonesian Borneo, The ecology of Indonesia series: vol. III, Periplus editions, Singapore, 1996. 7141

Mallela, J., Perry, C. T., and Haley, M. P.: Reef morphology and community structure along a fluvial gradient, Rio Bueno, Jamaica, Caribbean J. Sci., 40, 299–311, 2004. 7139

Mantel, S.: Berau model forest area environmental datasets and maps: land systems inventory, consultants report, DHV, BFMP, 2001. 7141

Marshall, A. J., Salas, L. A., Stephens, S., Nardiyono, Engstrom, L., Meijaard, E., and Stanley, S. A.: Use of limestone karst forests by Bornean orangutans (Pongo pygmaeus morio) in the Sangkulirang Peninsula, East Kalimantan, Indonesia, Am. J. Primatol., 69, 212–219, 2007. 7140

McLaughlin, C. J., Smith, C. A., Buddemeier, R. W., Bartley, J. D., and Maxwell, B. A.: Rivers, runoff, and reefs, Global Planet. Change, 39, 191–199, 2003. 7139

Merritt, W. S., Letcher, R. A., and Jakeman, A. J.: A review of erosion and sediment transport models, Environ. Modell. Softw., 18, 761–799, 2003. 7146

Meybeck, M., Laroche, L., Dürr, H. H., and Syvitski, J. P. M.: Global variability of daily total suspended solids and their fluxes in rivers, Global Planet. Change, 39, 65–93, doi:10.1016/S0921-8181(03)00018-3, 2003. 7151

Milliman, J. D. and Farnsworth, K. L.: River Discharge to the Coastal Ocean: A Global Synthesis, Cambridge university press, Cambridge, United Kingdom, first edn., 2011. 7139, 7154

Milliman, J. D., Farnsworth, K. L., and Albertin, C. S.: Flux and fate of fluvial sediments leaving large islands in the East Indies, J. Sea Res., 41, 97–107, 1999. 7139, 7154

Moehansyah, H., Maheshwari, B. L., and Armstrong, J.: Field evaluation of selected soil erosion models for catchment management in Indonesia, Biosystems Engineering, 88, 491–506, doi:10.1016/j.biosystemseng.2004.04.013, 2004. 7142

Morgan, R.: Soil erosion and conservation, Blackwell publishing, Oxford, England, 2005. 7163

Morgan, R. P. C. and Finney, H. J.: Stability of agricultural ecosystems: validation of a simple model for soil erosion assessment, Tech. Rep. cp-92-76, International institute for applied system analysis, Austria, 1982. 7163

Renard, K. G. and Freimund, J. R.: Using monthly precipitation data to estimate the R-factor in the revised USLE, J. Hydrol., 157, 287–306, 1994. 7147

Rogers, C.: Responses of coral reefs and reef organisms to sedimentation, Mar. Ecol. Prog. Ser., 62, 185–202, 1990. 7139

Schlax, M. G. and Chelton, D. B.: Frequency domain diagnostics for linear smoothers, J. Amer. Stat. Assoc., 87, 1070–1081, 1992. 7146

Spalding, M. D., Ravilious, C., and Green, E. P.: World Atlas of Coral Reefs, University of California Press, Berkeley, USA, London, England, 2001. 7139

Storms, J. E. A., Hoogendoorn, R. M., Dam, R. A. C., Hoitink, A. J. F., and Kroonenberg, S. B.: Late-Holocene evolution of the Mahakam delta, East Kalimantan, Indonesia, Sedimentary Geology, 180, 149–166, 2005. 7154

Syvitski, J. P. M., Vorosmarty, C. J., Kettner, A. J., and Green, P.: Impact of humans on the flux of terrestrial sediment to the global coastal ocean, Science, 308, 376–380, 2005. 7139

Tarya, A., Hoitink, A. J. F., and van der Vegt, M.: Tidal and subtidal flow patterns on a tropical continental shelf semi-insulated by coral reefs, J. Geophys. Res., 115, C09029, doi:10.1029/2010JC006168, 2010. 7140

Tarya, A., Hoitink, A. J. F., and van der Vegt, M.: Tidal control over river plume spreading in a near-equatorial region, J. Geophys. Res., submitted, 2011. 7140

Tomascik, T., Mah, A. J., Nontji, A., and Moosa, M. K.: The ecology of the Indonesian seas; Part One, The ecology of Indonesia series: vol. VII, Periplus editions, Singapore, 1997. 7139, 7140

Voss, F.: Kalimantan Timur Atlas, East Kalimantan Transmigration Area Development (TAD), Hamburg: Institut für Wirtschaftsforschung, Hamburg, Germany, 1982. 7141, 7142

Wischmeier, W. H. and Smith, D. D.: Predicting rainfall erosion losses- a guide to conservation planning, Agriculture Handbook no. 537, US department of Agriculture, Washington, 1978. 7147, 7153

Yu, B. and Rosewell, C. J.: A robust estimator of the R-factor for the universal soil loss equation, Trans. ASAE, 39, 559–561, 1996. 7147

Table 1. Forest cover (km^2) in time in the Berau district after Ekadinata et al. (2010).

	1995	2000	2005	2008
Undisturbed	12 196	8407	7551	4319
Logged-over	7121	7991	9497	5766
Total	19 317	16 398	17 048	10 085

Table 2. Overview of all measurements used for this study, which were taken at the cross section of Gunung Tabur.

Instrument	Period (Julian days from 1 January 2006)	Variables measured
HADCP	518–575	Flow velocity
OMS	503–548 and 612–630	Turbidity at one point
OBS*	507,510, 516, 620 and 628	Turbidity profiles

*During OBS profile measurements also water samples were taken to obtain suspended sediment concentration.

Table 3. Cover and management factors for various tropical land cover types (Morgan and Finney, 1982; Besler, 1987; Morgan, 2005).

Land cover type	C_m (–)
Primary rainforest	0.006
Secondary rainforest	0.002
Traditional shifting cultivation	0.001
Coffee (with cover crops)	0.1–0.3
Cacao (with cover crops)	0.1–0.3
Rubber	0.2
Oil palm (with cover crops)	0.1–0.3
Groundnut	0.2–0.8
Bare ground	1

Table 4. USLE factors for a hillslope that has characteristics typical for the Berau drainage basin, including R_e derived from rainfall during an average year and C_m that represents primary rainforest.

USLE factor	Value	Units
R_e	9820	$\mathrm{MJ\,mm\,ha^{-1}\,y^{-1}\,h^{-1}}$
K	0.013	$\mathrm{t\,h\,MJ^{-1}\,mm^{-1}}$
S_sS_l	2.8	
C_m	0.006	
P	1	

Table 5. Estimated annual soil loss per unit area from USLE for different land cover types. Other model input parameters are as specified in Table 4.

	A_e (t ha^{-1} y^{-1})
Primary rainforest	2.2
Oil palm without cover crops	108.1
Traditional shifting cultivation	0.4
Bare ground	360.3

Title Page
Abstract | Introduction
Conclusions | References
Tables | Figures
◄ | ►
◄ | ►
Back | Close
Full Screen / Esc
Printer-friendly Version
Interactive Discussion

Table 6. Rainfall for four different periods.

	P (mm y^{-1})
1987–2007	2105
6.5 weeks period	4080
2007	2762
Nov–Jan 1987–2007	2589

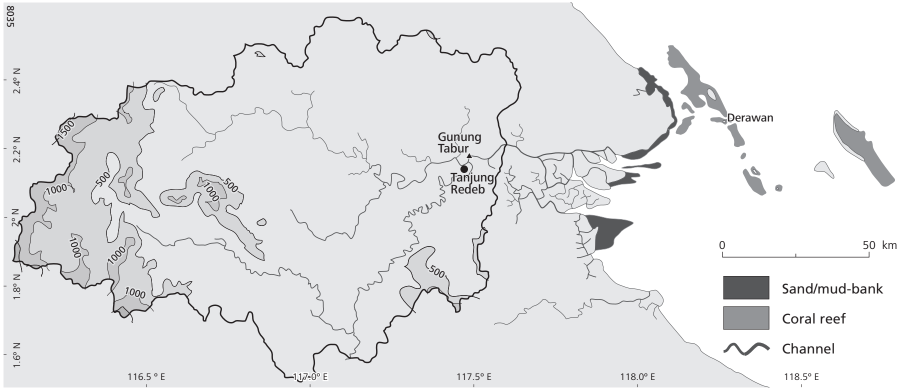

Fig. 1. Map of the Berau region showing the Berau river catchment with contour heights (m), the river and estuarine channels and the coral reef islands in the east.

Title Page
Abstract
Introduction
Conclusions
References
Tables
Figures
◀|
|▶
◀
▶
Back
Close
Full Screen / Esc
Printer-friendly Version
Interactive Discussion

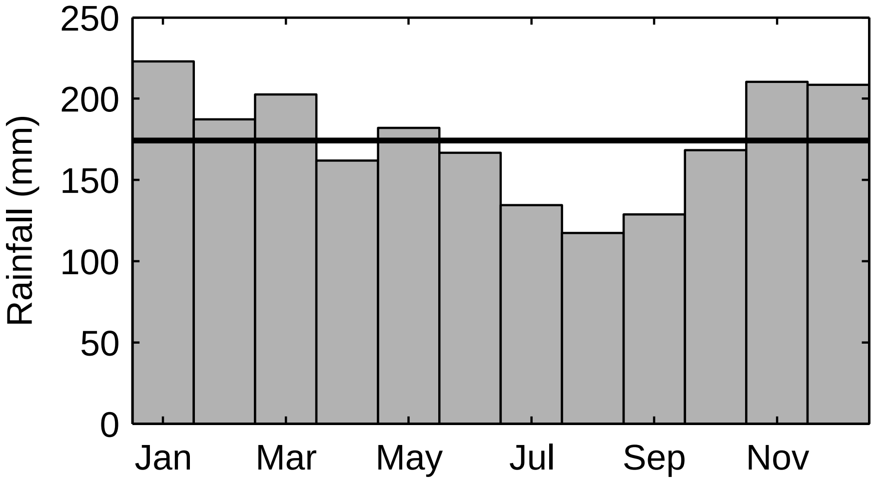

Fig. 2. Monthly rainfall at Tanjung Redeb based on the years 1987–2007. The yearly average is 2105 mm, which corresponds to an average monthly rainfall indicated by the thick line.

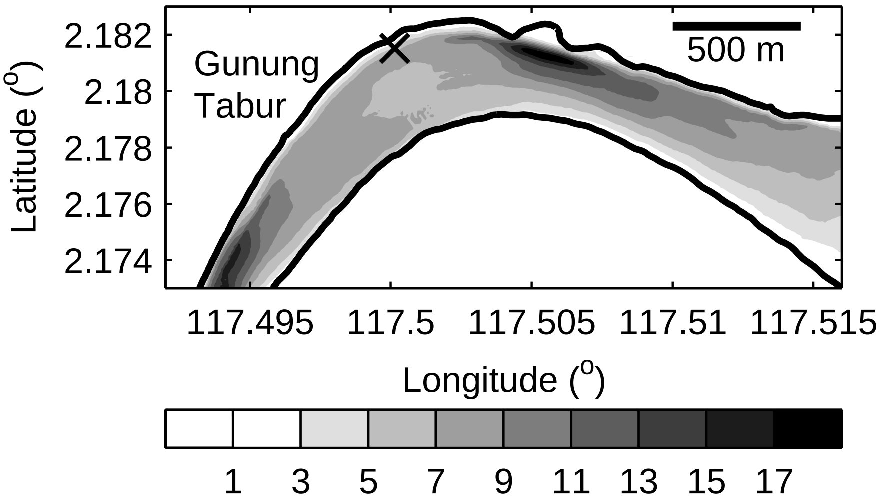

Fig. 3. Bathymetry of the Berau river close to the village Gunung Tabur showing depths with respect to mean water level (m). Instruments that obtain flow velocity and suspended sediment concentration were deployed at the location marked with an X.

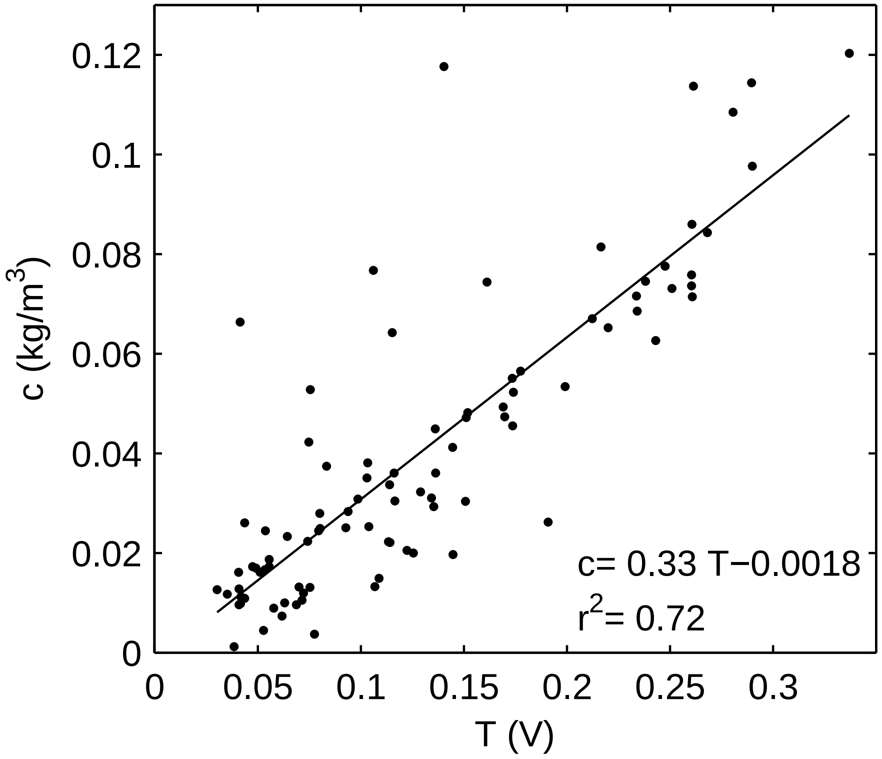

Fig. 4. Calibration of turbidity with total suspended matter (*c*) from in situ water samples.

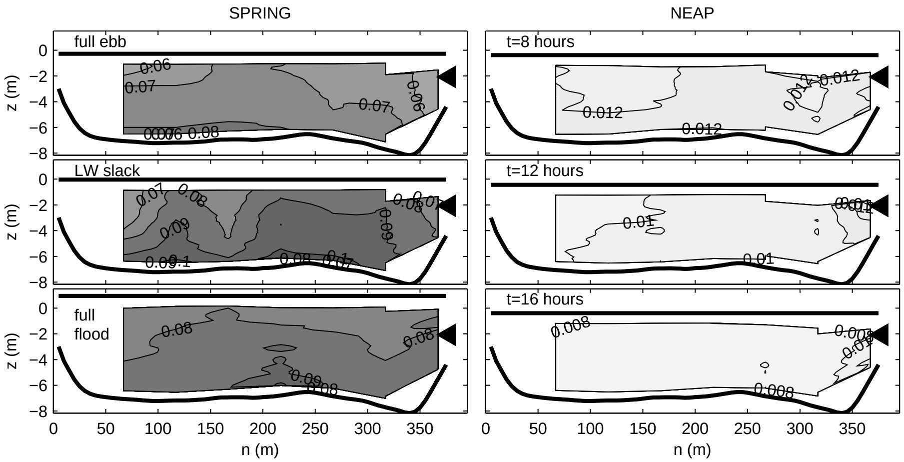

Fig. 5. Suspended sediment concentration from optical measurements (kg m^{-3}) in the cross section close to Gunung Tabur at three phases in a tidal cycle during spring tide [left] and during neap tide [right]. The black triangle indicates the position of the HADCP.

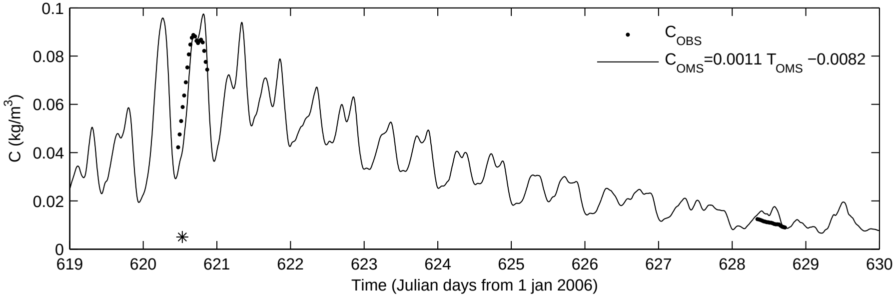

Fig. 6. Cross section averaged suspended sediment concentration for 11 days in September 2007.

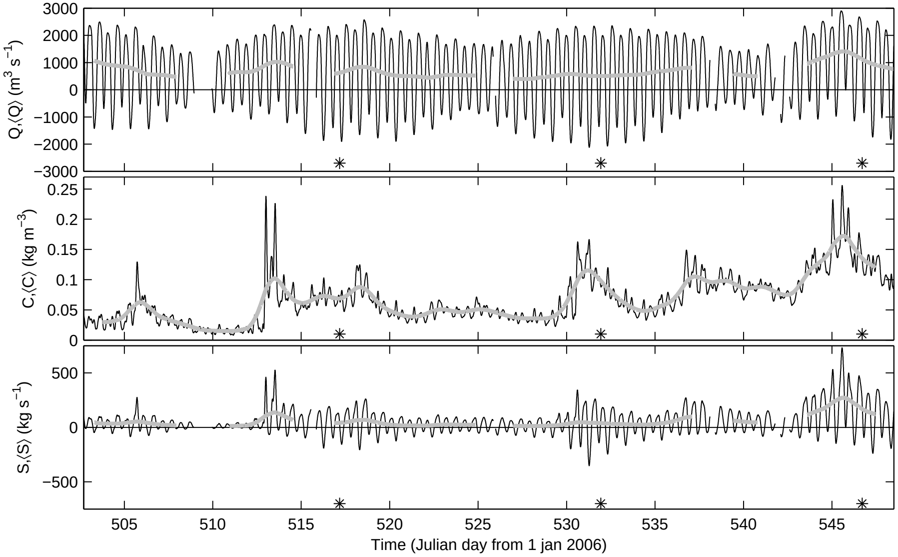

Fig. 7. Time series of discharge [top panel], of suspended sediment concentration averaged over the cross section [middle panel] and of suspended sediment flux [bottom panel]. The tidally average of these variables is indicated by thick grey lines and the stars indicate moments of spring tide.

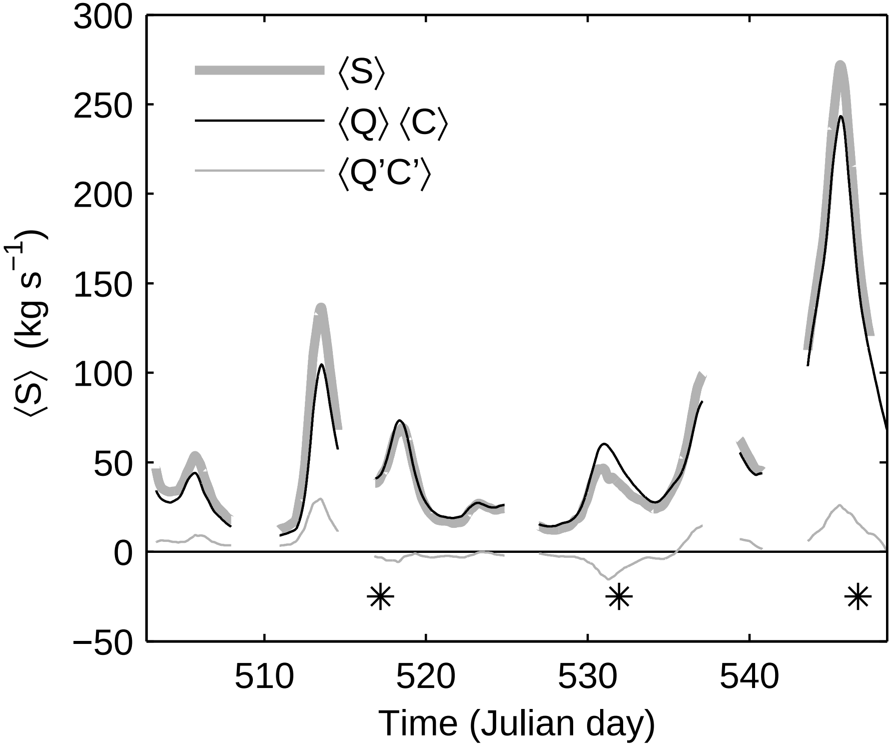

Fig. 8. Contribution of tidally averaged discharge and suspended sediment concentration, and contribution of varying discharge and suspended sediment concentration to tidally averaged suspended sediment flux.

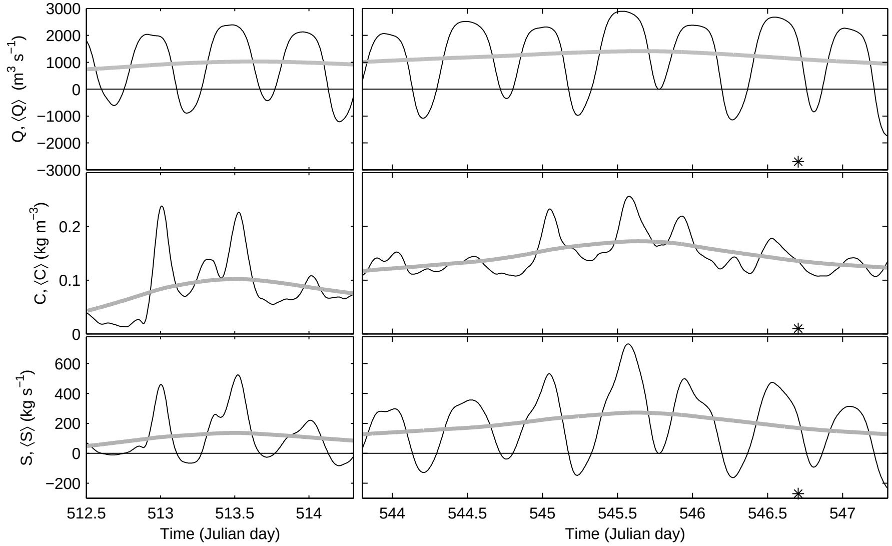

Fig. 9. As Fig. 7, now zoomed in on two periods with highest observed tidally averaged suspended sediment flux.